

# Effects of different hybrid electric architectures in fuel consumption and ethanol emissions for passenger cars

Vinícius Rückert Roso

Marcelo Rohrig

João Lucas Zaions

Jean Lucca Souza Fagundez

Thompson Diórdinis Metzka Lanza Nova

Mario Eduardo Santos Martins

Federal University of Santa Maria

## ABSTRACT

Electrification of the vehicular fleet is a worldwide tendency, considering both hybrid and fully electric solutions. However, many regional barriers hinder the dissemination of these technologies and the feasibility of their application, such as the production of electricity by non-renewable sources and the component costs. In this sense, hybrid platforms equipped with high efficiency internal combustion engines stand out as promising alternatives, even more when biofuels such as ethanol are used. As the hybridization concept is quite broad, different electric motor positioning and coupling architectures can enable operation exclusively by electric mode during parking conditions, cruising speeds, urban routes, among others. The aim of this paper is to evaluate different P0 and P2 hybridization architectures for a passenger car through computer simulation in GT-ISE software, considering experimental data of fuel consumption and engine-out emissions from an ethanol fueled Ford Ecoboost 1.0 l engine. The results show benefits of both architectures when compared to the baseline vehicle under urban driving cycles, pointing to advantages of lighter hybridization strategies which could be adapted to vehicles in production and offered as commercial packages by automakers.

## INTRODUCTION

In order to control global warming by reducing emissions from fossil fuels, several countries have adopted new policies and included legislation in order to renew their energy matrices so that they become more renewable [1]. The use of biofuels, such as ethanol, is already a reality, with mature production processes, a consolidated distribution network and good acceptance, reducing the total amount of carbon emitted due to the global cycle of production and use [2]. These renewable fuels, however, would always reach a limit of CO<sub>2</sub> reduction, without being able to avoid them completely.

As a way to further reduce or even eliminate carbon emissions, electrification of the propulsion system has proved to be the most viable solution. Even with the technology still under development, several automakers have bet on the total or partial electrification of their fleet,

incorporating the components in a significant portion of their commercial vehicles [3].

Electrification has reached the automotive scene in many ways, creating a series of different concepts that replace, to a lesser or greater extent, the vehicle's internal combustion engine (ICE) propulsion. The most common concept is the micro-hybrid, also known as start-stop, which automatically shuts off the engine in a situation of many stops (urban traffic), focusing on fuel economy [4]. Two other concepts that do not require electrical supply through an external source are the mild hybrid, with small battery packs and voltage that does not exceed 60V, and the full hybrid, with larger battery packs, electrical autonomy and voltages at the level of 250 ~ 300V [5]. These last two concepts charge their batteries only through braking energy recovery, among other recovery systems that work whenever the vehicle is in motion. Although its benefit in terms of economy and emission reduction is considerable, the electric range, even for full hybrids, is small [6]. So looking for solutions that add the reduction of carbon emissions provided by an electric vehicle and greater autonomy, which allows short trips, the plug-in hybrid or even a battery electric vehicle (BEV) are the options available [5][7]. But in addition to reducing fuel consumption and emissions, the transition to vehicles with a higher level of electrification also leads to smarter mobility, closely associated with artificial intelligence technologies, where traffic safety also becomes one of the most important factors [8].

By developing an analysis on a mild hybridization (MHEV) concept, several architectures for the location of the electric motor in the vehicle are possible. These locations can be seen in Figure 1.

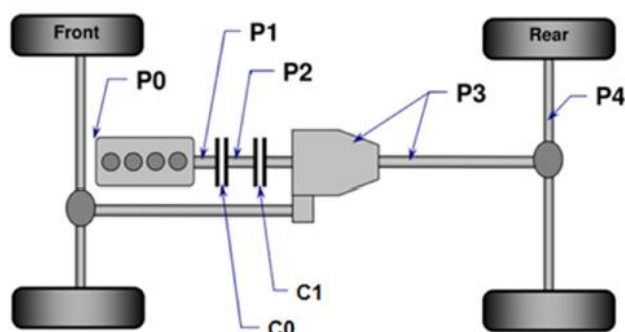


Figure 1. Several hybrid architectures for the electric motor position, from P0 to P4 [5] - Adapted.

Although some architectures have a similar position of the electric motor, such as P1 and P2, their application complexity is completely different, since the P2 architecture is coupled to the transmission, between the clutches, and the P1 architecture places the motor between ICE and transmission [4]. The P0 architecture, on the other hand, is the most commonly used and has been on the market the longest. Its application is mainly by activating vehicle components and accessories through recovered energy, without the need to use work from the ICE. It is often called a belt alternator starter (BAS). The P3 and P4 architectures have the electric motor placed after the gearbox and their complexity can vary. In the P4 architecture, for example, it is possible to configure a central electric motor on the rear axle, if the front axle is that of the ICE, as well as to place independent motors on the vehicle's wheels (hub motors) [4][9].

The objective of this paper was to compare the possible gains in terms of fuel consumption and emission reduction with the application of the P0 and P2 architectures, configured for the electric machine of a mild hybrid, against a conventional vehicle with a Ford EcoBoost 1.0 l engine fueled with ethanol. For this purpose, consumption maps and brake mean effective pressure (BMEP) were used to determine the vehicle's operating baseline in the GT-ISE software [10]. Both the vehicle with baseline setup (ICE only) and its hybrid versions P0 and P2 were tested using the FTP-75 urban emissions driving cycle [11] as a reference.

## METHODOLOGY

This investigation was carried out in two stages, considering experimental tests to provide operation maps of the internal combustion engine (ICE) and also the development of computational models to implement this engine in different operation strategies of hybrid vehicles. The following sections present the materials and methods involved in each of these steps.

## EXPERIMENTAL SETUP FOR ICE ANALYSIS

A three cylinder turbocharged Ford EcoBoost engine was coupled in a dynamometric bench to provide the fuel consumption and exhaust emission maps. Table 1 presents

the specifications of the engine and of the Brazilian ethanol considered in the experimental tests.

Table 1. Ford EcoBoost engine and Brazilian ethanol specifications

Engine specification		
Displacement	cm <sup>3</sup>	998
Bore	mm	71.9
Stroke	mm	82
Compression ratio		10.0:1
Max Power	kW	74 (at 4500 rpm)
Max Torque	Nm	170 (at 4000 rpm)
Number of cylinder		3
Fuel injection type		High pressure direct fuel injection with 6 hole injectors
Turbocharger		Continental low inertia turbo
Valve gear		DOHC with 4 valves per cylinder, twin independent variable cam timing
Ethanol specification		
Density	kg/m <sup>3</sup>	808.7
Carbon	%m/m	48.8
Hydrogen	%m/m	13
Oxygen	%m/m	38.2
Molar ratio	H/C	3
Ethanol	%v/v	95.7
Water	%v/v	4.3
Stoichiometry		8.8
LHV	MJ/kg	25.27

Ignition and fuel injection parameters were set through a Bosch Motorsport MS 6.3 open ECU to achieve maximum brake torque conditions and stoichiometric operation, respectively. Camshaft positions were evaluated symmetrically every 10°CA looking for the condition of highest indicated efficiency in each operating condition. Furthermore, during the calibration procedure, the in-cylinder pressure was maintained below 100 bar to preserve engine integrity, which was achieved by limiting turbocharger and fuel injection pressures.

Intake and exhaust pressures were monitored using MPX4250 and AVL APT100 pressure transducers, respectively. Exhaust gas temperatures, before and after turbine, oil reservoir and cooling system were monitored with type K thermocouples. Atmospheric pressure, temperature and air humidity were measured using a VAISALA HMT330 unit. An AVL GH14D piezoelectric

pressure transducer and the AVL IndiMicro 602 system were used to acquire and process the in-cylinder pressure data. Online combustion analysis was performed using AVL Indicom software. Engine load was applied using a AVL DynoPerform 240 dynamometer, with torque measurements with a HBM T40B torque flange. Ethanol mass flow was measured through a Endress Hauser Promass A200 Coriolis, while the concentration of engine-out emissions was measured with a AVL Sesam FTIR i60 gas analyzer. AVL Puma Open system was simultaneously used to control the actuators of the test cell and for data acquisition.

Average of instantaneous in-cylinder pressure was calculated from 200 cycles, while the pressure transducers, thermocouples and gas analyzer performed measurements for 30 seconds and then an arithmetic average was taken. Also, 10 seconds were considered for stabilization before gas analyzer triggering, to ensure continuous flow between the exhaust pipe and the gas measurement cell.

As input data for the computational model, experimental maps of the ICE operation were performed considering different operating regimes. Figure 2 shows the stationary points used in the interpolation of these operational maps. Such data include operation at idle condition and 6 load points at 3 different engine speeds, covering the full extent of the operation map.

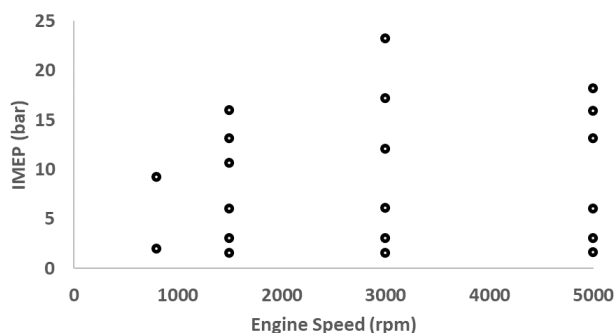


Figure 2. Experimental operating points that were considered in the vehicle simulation.

## HYBRID ARCHITECTURE SIMULATIONS

Under FTP-75 driving cycle, two vehicular hybrid architectures were compared to the conventional baseline vehicle, powered only by the internal combustion engine, considering computer simulation in GT-Power software. Table 2 shows the model input data from a Ford Fiesta Ecoboost, which is the vehicle equipped with the engine tested on the dynamometric bench.

Table 2. Vehicle specifications.

Kerb Weight (kg)	1164
Wheelbase (mm)	2493
Overall length (mm)	4040
Tires	205/45/17
Cd	0.3
A (m <sup>2</sup> )	2.15
Gear ratios	1st - 3.417
	2nd - 1.958
	3rd - 1.276
	4th - 0.943
	5th - 0.757
	6th - 0.634
Final drive ratio	3.941

Based on the vehicle's mass, aerodynamic coefficients and transmission ratio, the model calculates the torque required by the vehicle to reach certain speed gradients. With this, the maps of engine speed and torque are interpolated and then the fuel consumption and engine-out emissions, also inserted from experimental tests, are obtained. Thus, computational errors are minimal, since the calculations performed by the software are limited to the required engine speed and torque. These simulations did not consider gains in transient conditions, and a direct linear interpolation of the experimental data in steady state was performed.

To make the vehicle a P0 mild hybrid, a small BAS motor with 28 kW was attached to the engine to give the start-stop capability. The motor is powered by a 4.7 A-h battery. With the vehicle stopped and the ICE turned off, there is a demand for torque through the accelerator and then BAS actuates to start the vehicle movement. Regeneration occurs during deceleration events, until the vehicle stops again and the ICE is turned off. However, the ICE is only turned off if the batteries are sufficiently charged to restart the system. For the simulation, initial SOC was assumed to be of 70% of battery capacity.

In the P2 model, an electric motor is positioned between the engine and the transmission with a clutch system on each side. With this, the electric machine could provide direct propulsion to the vehicle, assist the ICE with propulsion or actuate as a generator. The first clutch, between the engine and the electric machine, is engaged during starts, engine propulsion and series-hybrid operation. The second clutch, between the electric machine and the transmission, is engaged during all driving and regenerative braking events. The motor is powered by an 8 A-h battery, which starts the simulation with 65% of its capacity. As an operating strategy, it was considered that, if the battery charge state is greater than 35%, the operation takes place only in electric

mode. If it decreases from that, the vehicle operates in a hybrid mode until the SOC present higher values. Thus, the engine will start when the vehicle speed exceeds values defined by a SOC versus speed relation or when the tractive power demand is greater than the maximum power limit of the electric machine, remaining on or off for at least 3 or 2 seconds, respectively. For the hybrid operation, gear shift strategies considered an optimized strategy for FTP-75 driving cycle, being the gear up-shifts occurring at 20 (1<sup>st</sup>-2<sup>nd</sup>), 29 (2<sup>nd</sup>-3<sup>rd</sup>), 47 (3<sup>rd</sup>-4<sup>th</sup>), 66 (4<sup>th</sup>-5<sup>th</sup>) and 90 km/h (5<sup>th</sup>-6<sup>th</sup>).

## RESULTS

The results were divided into three subsections: the first showing the difference of each vehicle architecture to the ICE speed in the FTP-75 cycle; the second for hybrid architectures battery usage during the FTP-75 cycle; and the third for the comparison of specific fuel consumption and emissions between the conventional vehicle and the hybridizations P0 and P2.

### FTP-75 DRIVING CYCLE ANALYSIS

The graph in Figure 3 shows the ICE speed profiles during the FTP-75 driving cycle for the vehicle with baseline configuration and with P0 and P2 hybrid architectures.

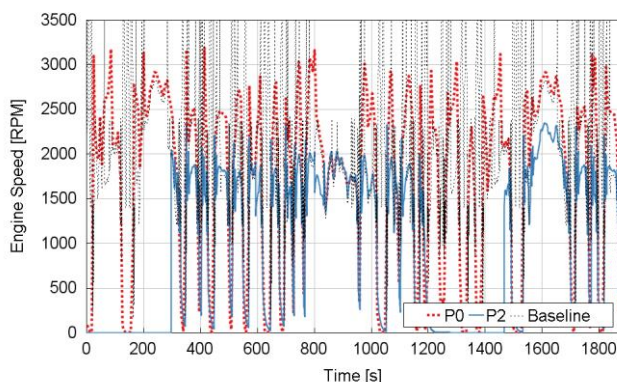


Figure 3. Engine speed of the internal combustion engines during the FTP-75 driving cycle with P0 and P2 hybrid architectures.

It is possible to notice, through the speed profiles, that the vehicle with baseline setup, that is, only with ICE, was the one that reached the highest engine speeds throughout the entire cycle. More than that, using a hybrid architecture prevents the engine from reaching higher speeds along the entire cycle.

Hybridization with P0 architecture keeps the internal combustion engine in use throughout the cycle, as it does not allow electrical autonomy, only aids in the torque delivery. On the other hand, the P2 architecture avoids the use of ICE

in occasions when poor efficiency occurs, such as idling and low speeds. This can be seen in the range of 0 to 300 seconds and at times between 1200 and 1400 seconds. Also, when the ICE is used, the electric motor torque delivery is higher and the engine speed can be lower.

### STATE OF CHARGE COMPARISON

The battery state of charge (SOC) of each hybrid architecture was shown along the FTP-75 driving cycle in Figure 4.

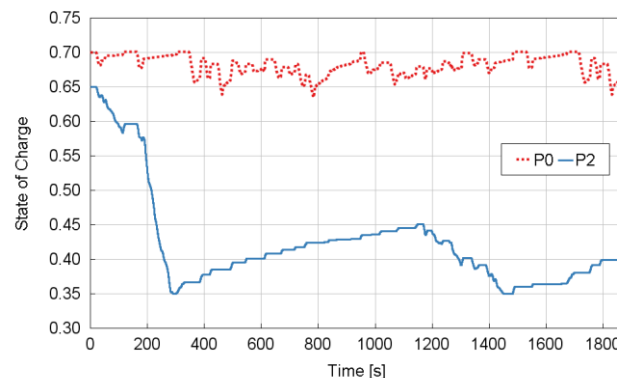


Figure 4. State of charge of the battery packs during the FTP-75 driving cycle with P0 and P2 hybrid architectures.

Figure 4 shows important information about the batteries SOC of each hybrid architecture during the investigated cycle. The P0 architecture maintains a nearly constant state of charge for the duration of the test, between 60 and 70% of the full load. Its use occurs occasionally, reducing the need for the ICE. The P2 architecture has a very different profile because, when it is used intensively, at the beginning of the cycle, the battery charge decreases from 65% to 35%, with a gradual recharge as the ICE starts to be used.

### HYBRID ARCHITECTURE IMPACT ON BSFC AND EMISSIONS

Following are the response surface graphs comparing the impact of using hybrid architectures on brake specific fuel consumption (BSFC) and vehicle emissions. For this, are considered the ICE operation points of each strategy over the FTP-75 driving cycle. In Figure 5 the response surface with the BSFC comparison is shown.

In the BSFC map is observed a reduction in the values for partial loads, between 10 and 16 bar of BMEP, due to a greater efficiency of gas exchange and the reduction of pumping losses due to the dethrottling condition, with less restriction by the throttle valve. Until these conditions, the engine is in naturally aspirated operation, with load being controlled by throttle position. After that, engine load is increased through the boosting pressure. As the throttle is closed to reduce engine load, pumping losses tend to increase, resulting in an increase in specific fuel consumption. With this trend, an optimization in BSFC for

P2 hybrid strategies can be obtained if the ICE operates under full load conditions of the naturally aspirated region, optimizing the fuel use for power generation and consequently, for electric operation. The P0 architecture also presents good results in urban cycles especially by preventing the engine from operating in idle conditions.

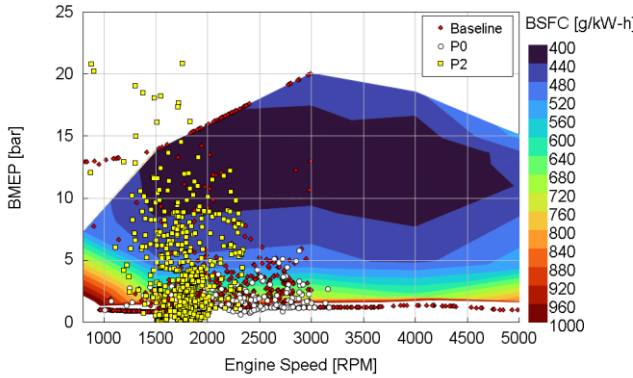


Figure 5. BSFC in terms of BMEP and engine speed for baseline, P0 and P2 setups.

As a result of incomplete oxidation of the fuel, CO emissions occur mainly due to rich air-fuel mixtures or difficulties of homogenization. In this sense, it is expected that at higher engine speeds the homogenization of the mixture will benefit, reducing CO levels as shown in Figure 6. On the other hand, for rich mixtures such as those adopted to control exhaust temperature at high engine loads and speeds, there is not enough oxygen to completely burn all the carbon contained in the fuel and form CO<sub>2</sub>, resulting in CO formation. The three evaluated strategies presented good positioning of the operating points, which may present benefits if the speed range in which the ICE operates is extended.

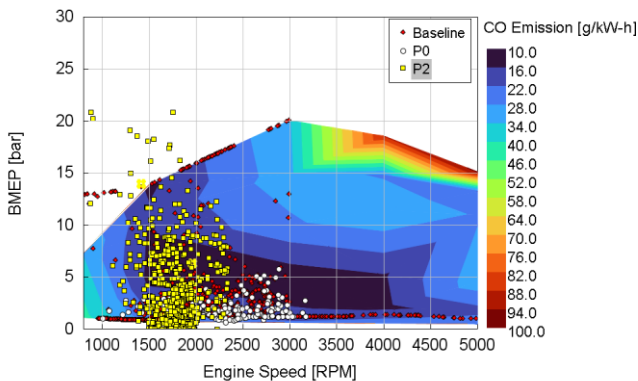


Figure 6. CO emissions in terms of BMEP and engine speed for baseline, P0 and P2 setups.

Emissions of unburned hydrocarbons (HC) are potentiated especially when there is incomplete fuel combustion or when the temperature involved is relatively low to complete the reaction, which can result in flame extinguishing. Thus, high temperatures in the combustion chamber, as those observed

in high load conditions, tend to reduce the temperature difference between the gases and the chamber, resulting in less heat transfer between the mixture and the cylinder walls. The opposite behavior shown in Figure 7 for high loads can be attributed to engine wear, whether in piston rings or in turbocharger, resulting in the burning of lubricating oil and consequent increase in HC emissions. Thus, for this condition, the distribution of operating points is satisfactory as it is away from regions of higher HC emissions.

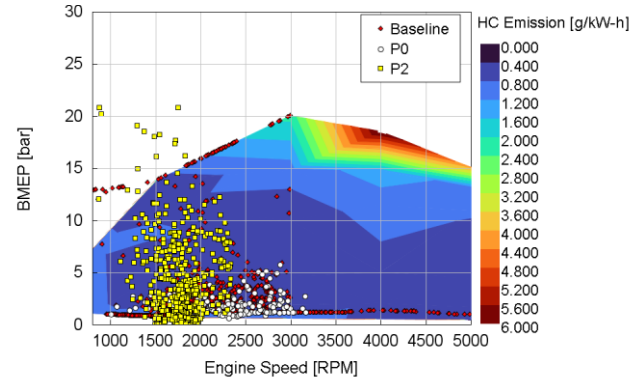


Figure 7. HC emissions in terms of BMEP and engine speed for baseline, P0 and P2 setups.

During the combustion process, the amount of NO<sub>x</sub> formed by an engine is directly related to the in-cylinder temperature and the combustion duration. At high loads, it is possible to observe an increase in NO<sub>x</sub> emissions due to the high fuel demand to maintain the stoichiometric air-fuel mixture, consequently raising in-cylinder pressure. As shown in Figure 8, when the mixture is enriched to control the maximum cylinder pressures, as those above 14 bar of BMEP and 5000rpm, the in-cylinder temperature is reduced due to the excess of fuel, which consequently reduces NO<sub>x</sub> emissions. In this sense, the P0 presented a greater reduction if compared to the P2, especially due to the operation in a wider range of engine speed and at lower loads, not entering the region of higher NO<sub>x</sub> emissions.

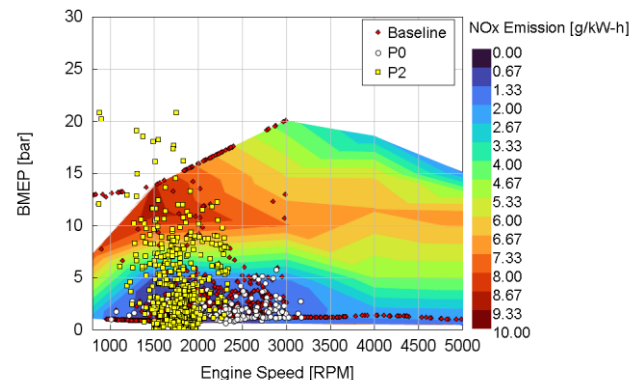


Figure 8. NO<sub>x</sub> emissions in terms of BMEP and engine speed for baseline, P0 and P2 setups.



Table 3 shows a summary, with the comparison between the average values of BSFC and emissions. One can clearly see the impact of reducing fuel consumption through the use of hybrid architectures. When using a BAS (P0), the vehicle had a consumption, in g/km, about 42.5% lower in the FTP-75 cycle. In the P2 architecture, the difference is even greater, with a reduction of around 48% in consumption compared to the conventional vehicle.

Table 3. Average of fuel consumption and engine-out emissions over FTP-75 driving cycle with P0 and P2 hybrid architectures and the baseline ICE vehicle

Variable	Unit	Baseline	P0	P2
Fuel consumption	g/km	152,59	87,84	79,13
CO	g/km	5,30	2,01	1,33
HC	g/km	0,23	0,08	0,05
NOx	g/km	0,96	0,20	0,36

The reduction in emissions, in g/km, is also quite significant. With any of the hybrid architectures tested, emissions are reduced by more than 50% for the FTP-75 cycle. The P2 architecture is the one that obtained the lowest values for CO and HC emissions, while P0 reached the lowest NOx emission. This difference is consistent, as lower CO and HC emissions indicate higher combustion efficiency, which in general leads to higher in-cylinder temperatures and increased NOx formation.

The results achieved help to understand the new appeal of the automotive industry towards hybrid and electric vehicles. In the Brazilian scenario, which still has a small infrastructure for electric supply, MHEV or FHEV vehicles gain more space. Even mild hybridizations are able to show a significant impact on consumption and emissions, making renewable fuels such as ethanol more competitive and giving an important lifespan to internal combustion engines, by reducing their carbon footprint.

## CONCLUSIONS

This investigation presents a comparative study of P0 and P2 hybrid architectures when applied to a commercial vehicle, comparing with the baseline vehicle powered exclusively with ICE. By the methodology used and the results obtained, the main conclusions are that:

- The combination of experimental data from ICE with the implementation of hybridization logics in simulation software points to a feasible and reliable methodology to evaluate architectures and strategies;
- Both hybrid strategies have the potential to reduce fuel consumption and exhaust emissions in urban applications. These architectures may present even greater benefits in other driving cycles, especially those that consider large numbers of stops or intense traffic conditions;
- Optimization in gear shift events and energy management could improve the results, positioning the ICE operation in the most efficient regions of engine map;
- P0 architectures can be an extremely viable hybrid option, since it presents good results with lower application costs.

The authors would like to thank the Rota2030-FUNDEP program and Marelli Sistemas Automotivos for funding this research.

## REFERENCES

- [1] S. R. Sinsel, R. L. Riemke, and V. H. Hoffmann, "Challenges and solution technologies for the integration of variable renewable energy sources—a review", *Renewable Energy*, vol. 145, pp. 2271–2285, 2020.
- [2] M. Mourad and K. Mahmoud, "Investigation into engine performance characteristics and emissions fuelled with ethanol/butanol-gasoline blends", *Renewable Energy*, vol. 143, pp. 762–771, 2019.
- [3] B. Sarlioglu, C. T. Morris, D. Han, and S. Li, "Benchmarking of electric and hybrid vehicle electric machines, power electronics, and batteries," in 2015 Intl Aegean Conference on Electrical Machines & Power Electronics (ACEMP), 2015 Intl Conference on Optimization of Electrical & Electronic Equipment (OPTIM) & 2015 Intl Symposium on Advanced Electromechanical Motion Systems (ELECTROMOTION). IEEE, 2015, pp. 519–526.
- [4] C. Mi, M. A. Masrur,, "Hybrid Electric Vehicles - Principles and Applications with Practical Perspectives", Second Edition, John Wiley & Sons Inc., 2018.
- [5] A. English, T. Pfund, D. Reitz, E. Simon, F. Kolb, "Synthesis of various hybrid drive systems", *Der Antrieb von morgen*, pp. 61 - 78, 2017.
- [6] N. D. S. A. Santos, V. R. Roso, M. T. C. Faria, "Review of engine journal bearing tribology in start-stop applications", *Engineering Failure Analysis*, vol. 108, 104344, 2020.
- [7] N. D. S. A. Santos, V. R. Roso, A. C. T. Malaquias, J. G. C. Baêta, "Internal combustion engines and biofuels: Examining why this robust combination should not be

ignored for future sustainable transportation”, *Renewable and Sustainable Energy Reviews*, vol. 148, 11292, 2021.

[8] M. Nikowitz, “Advanced Hybrid and Electric Vehicles - System Optimization and Vehicle Integration”, *Lecture Notes in Mobility*, Springer, 2016.

[9] M. Ehsani, Y. Gao, J. M. Miller, "Hybrid Electric Vehicles: Architecture and Motor Drives," *Proceedings of the IEEE*, vol. 95, no. 4, pp. 719-728, 2007.

[10] GT-Suite v2021, Vehicle Hybrid Electric, Gamma Technologies.

[11] US EPA, “Dynamometer Drive Schedules”, accessed in May 15th, 2022, in: <https://www.epa.gov/vehicle-and-fuel-emissions-testing/dynamometer-drive-schedules#FTP>.